Determination of Equation-of-State Parameters by Molecular Simulations and Application to the Prediction of Surface Properties for Polyethylene

Won Ho Jo* and Kyoungsei Choi

Department of Fiber and Polymer Science, Seoul National University, Seoul 151-742, Korea

Received January 12, 1996; Revised Manuscript Received October 16, 1996[⊗]

ABSTRACT: By combination of an equation-of-state (EOS) theory and molecular simulation methods, a new way to predict and to analyze the surface phenomena of polymeric materials is suggested. The EOS parameters, p^*, v_{sp}^* and T^* of polyethylene are calculated by molecular simulation methods, without any experimental effort. With the calculated parameters, surface tensions and density profiles at surface are obtained by numerically integrating Poser and Sanchez's equations. The calculated surface tensions without adjustable parameters are slightly underestimated as compared to the experimental measurements. The underestimation may come from the fact that the simulated densities are lower than the experiments and that the EOS parameters are practically functions of temperature.

Introduction

In recent years, molecular simulation methods such as molecular mechanics (MM), molecular dynamics (MD), and Monte Carlo simulation (MC) have been applied to several polymer systems.[1−4] The method becomes a powerful tool in polymer science, complementing both analytical theory and experiment, but at the same time it has a serious limitation in the space and time scale it can cover. Many phenomena of polymers have a much larger scale in space and a longer scale in time than those the molecular simulation can directly deal with. In spite of the magnificent progress of computing power, it has not yet been feasible to treat polymers with more than ten thousand atoms in a system for longer than 1 ns in full atomistic MD.

Some alternatives have been developed to overcome the problems. Many physical properties of polymeric materials such as viscoelasticity, phase separation behavior, tensile strength, and self-diffusion are less sensitive to the exact chemical structure of monomers. Instead, the physical geometry or the molecular weight of polymers is more closely related with the properties. Thus, a polymer molecule can be simplified to have only a few interaction sites and/or to follow an ideal motion on a lattice space according to the reptation, the pivot algorithm, or the bond fluctuation method, when research interests are confined to the physical properties. The coarse-grained lattice model[5] has been successful in extending the scope. The model, however, does not include detailed information on the structure of materials and thus will be fictitious. Hence, some efforts were made to assign molecular parameters to the effective subunits in the coarse-grained lattice model.[6] The force field of another coarse-grained off-lattice model[7] has been developed by first simplifying the structure intuitively and then imposing several potential functions related to the bond stretching and nonbonded van der Waals interactions. The polymer reference interaction site model (PRISM) theory has been also employed to study the miscibility of polymer blends on the basis of the coarse-grained model.[8] In addition, phase diagrams have been predicted by the Flory−Huggins theory combined with molecular simulations by which the interaction parameters and coordination numbers were evaluated.[9,10] In short, a simplified coarse-grained modeling or a molecular simulation combined with a theory based on statistical mechanics is essential to investigate large-scale dependent properties of polymers.

The equation-of-state (EOS) theory for polymers has been developed as a useful tool to give information on equation-of-state properties,[11] and it enables us to predict the surface tensions, phase stability of polymer blends, etc. A pure polymer is characterized by three characteristic parameters, p^*, v^* and T^*, from which the thermodynamic properties can be deduced using the EOS theory. In case of polymer mixtures, the EOS theory includes the free volume term unlike the Flory−Huggins theory and describes the LCST as well as the UCST. The theory, however, requires tedious experiments to determine the characteristic parameters when dealing with a new polymer. Thus, it will be helpful if molecular simulation methods can provide the characteristic parameters without experimental efforts.

As an exploratory work to combine the EOS theory for surface tension and the molecular simulation methods, the characteristic parameters were first determined by molecular simulations, and then the surface tensions and the density profiles at surface for linear polyethylene (PE) were predicted according to Poser and Sanchez's approach[12,13] and compared with experimental results.

Theory

For polymer liquids, the gradient approximation in conjunction with the lattice fluid (LF) model has been used to calculate surface tensions.[12−14] For the LF model the chemical potential is given by

$$\tilde{\mu} = -\tilde{\rho} + \tilde{p}\tilde{v} + \tilde{T}\frac{(1-\tilde{\rho})\ln(1-\tilde{\rho})}{\tilde{\rho}} + \frac{\ln\tilde{\rho}}{r} \qquad (1)$$

where ρ is density, p is pressure, v is volume, T is temperature, and r is molecular size parameter. The chemical potential, density, pressure, and temperature are reduced by their respective characteristic parameters as follows:

$$\tilde{\mu} = \frac{\mu}{rNkT^*},\ \tilde{\rho} = \frac{\rho}{\rho^*} = \frac{1}{\tilde{v}},\ \tilde{p} = \frac{p}{p^*},\ \tilde{T} = \frac{T}{T^*} \qquad (2)$$

* To whom correspondence should be addressed.
[⊗] Abstract published in *Advance ACS Abstracts,* March 1, 1997.

S0024-9297(96)00041-1 CCC: $14.00

Table 1. Model Description

	calculation of long-range interaction		inclusion of Coulomb force
	spline	Ewald	
model A	×		
model B		×	
model C		×	×

Assuming high molecular weight ($r \rightarrow \infty$) and near atmospheric pressure ($\tilde{p} \rightarrow 0$), the chemical potential is simplified as

$$\tilde{\mu} = -\tilde{\rho} + \tilde{T}\frac{(1-\tilde{\rho})\ln(1-\tilde{\rho})}{\tilde{\rho}} \tag{3}$$

The density profile can be determined by integrating the Euler−Lagrange equation

$$\tilde{x} - \tilde{x}_0 = \int_{\tilde{\rho}_0}^{\tilde{\rho}_l} (\tilde{\kappa}/\Delta\tilde{a})^{1/2}\, \mathrm{d}\tilde{\rho} \tag{4}$$

where the subscripts 0 and l denote an arbitrary reference point and liquid state, respectively, x is a position along the line vertical to the surface, and $\tilde{\kappa}$ is a dimensionless constant. The $\tilde{\kappa}$ can be expressed as $\tilde{\kappa} = \tilde{\kappa}_1 + \tilde{\kappa}_2(\tilde{T}/\tilde{\rho})$ where *a priori* theoretical values of $\tilde{\kappa}_1$ and $\tilde{\kappa}_2$ are $^1/_2$ and $^1/_{36}$, respectively.[12] The Cahn−Hilliard relation for surface tension σ, in terms of reduced variables, can be expressed as

$$\tilde{\sigma} = 2\int_{\tilde{\rho}_g}^{\tilde{\rho}_l} (\tilde{\kappa}\Delta\tilde{a})^{1/2}\, \mathrm{d}\tilde{\rho} \tag{5}$$

where

$$\Delta\tilde{a} = \tilde{\rho}[\tilde{\mu}(\tilde{\rho}, \tilde{T}) - \tilde{\mu}(\tilde{\rho}_l, \tilde{T})] \tag{6}$$

$$\tilde{\sigma} = \frac{\sigma}{(kT^*)^{1/3}(p^*)^{2/3}},\ \tilde{x} = \frac{x}{(v^*)^{1/3}} \tag{7}$$

In eq 5, the subscript g denotes gas state. By substituting eq 3 into eq 6 and then integrating eq 4 and eq 5, the density profile and the surface tension can be obtained, respectively.

Model and Simulation

The commercial software *Cerius*[2] from Molecular Simulations Inc. is used and the force field UFF[15] is adopted in this work. The monomeric units of a fully atomistic PE are modeled to have a total charge of zero, and the distribution of the partial charge in the monomer is determined by the charge equilibration method (QEq).[16] They are polymerized to have a linear architecture, and then a single PE chain (C_{200}) with 100 monomeric units is packed into a simulation box which has 3-dimensional periodicity. The reason why a single chain, instead of multiple shorter chains, is introduced into our system is to eliminate the unusual distribution of free volumes due to many chain ends. The interaction sites in a chain interact with their images as if another chain was there. The intramolecular interactions may be described by terms such as bond, bending, and torsion energy; the intermolecular interactions by terms such as van der Waals and electrostatic energy. Three types of model systems are built depending upon the calculation methods of long-range interactions (Table 1). For example, model B does not include the electrostatic energy, and the remaining nonbonded interaction, i.e. van der Waals energy, is calculated using the Ewald method.[1] The exclusion of the electrostatic energy may be justified because PE is a nonpolar molecule. For the spline method, a spline function is multiplied to correct the discontinuity in the forces and potentials at a cutoff distance. This is a simple and fast method to calculate van der Waals and electrostatic terms, but may cause significant errors when the long-range energy—the attractive part of the van der Waals energy and the electrostatic energy—becomes important at above the cutoff distance. Hence, a long-range correction is essential in this method.

Six different structures are initially generated by the rotational isomeric state (RIS) algorithm and relaxed to avoid the overlaps between atoms. Then the structures are annealed to a higher temperature (1000 K) and cooled to 300 K repeatedly to overcome the local minimum energy barriers using an *NVT*-MD algorithm. At the end of each cycle the structures are relaxed by MM, allowing the length parameters of the cell to vary.

From the fully relaxed model polymers an isothermal−isobaric MD (*NpT*-MD)[17] starts, the temperature is lowered from 300 to 50 K at intervals of 50 K, and then the information at 0 K is collected by extrapolating the volumetric and energy data to 0 K. The MD run at each temperature is performed for 50 000 steps, where a time step is set to 1 fs. The equilibration at each temperature is monitored by the total energy and the volume of the simulation box.

The MM is also used to obtain equilibrium structures at 0 K. Starting from the fully relaxed structures by MD, both the coordinates of atoms and the cell parameters are energy-minimized to obtain the close-packed state.[18,19] Six initial models for MM runs are extracted from the six MD results performed at 300 K.

In summary, the volume-temperature and the energy-temperature data are collected from the results of the *NpT*-MD, and the energy-minimized state at 0 K is directly obtained from the MM. The characteristic parameters are then obtained by a simple analysis of the simulation results.

Results and Discussion

The model polymers produced by both MD and MM are in an amorphous state as can be confirmed by the radial distribution function (RDF) and the bond orientation function. There are no remarkable peaks above 5 Å in the RDF, and the bond orientation function vanishes as the MD runs develop, implying that there are no long-range orders in our model systems. It is well-known that PE is easily crystallizable. However, an amorphous state is rather usual for full atomistic molecular simulations because the available run time is too short to observe the significant diffusions and rearrangements of polymer chains. If one wishes to prepare a PE crystal from an amorphous state, another algorithm, whether it is dynamic or not, is needed to guarantee the fast relaxation of polymer chains, or nonperiodic conditions should be given to allow more free motion.

The equilibration of MD is monitored by the time evolution of density and total energy. As shown in Figures 1 and 2, the density reaches an equilibrium value at about 30 ps and then fluctuates around an average value, while the energy reaches an equilibrium very fast without a significant fluctuation. It is noteworthy that the difference between the 50 and 200 ps run MD results for the density and energy is negligibly small. Moreover, we have also observed that the

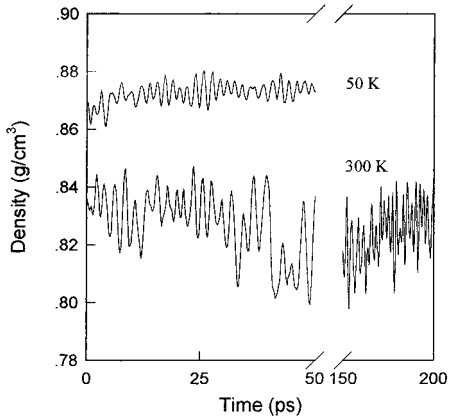

Figure 1. Time evolution of densities when the MD is performed for model A. The data for the other temperatures are omitted for clarity.

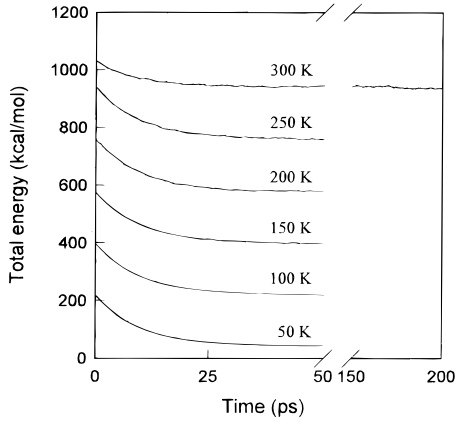

Figure 2. Time evolution of total energies when the MD is performed for model A.

distribution of torsional angles is symmetric at 50 ps run and that the symmetry is retained at lower temperatures. Therefore, the MD simulations longer than 50 ps are not necessary to give more accurate data for our system.

The *NpT*-MD performed here gives the information on the temperature dependence of several properties. All the simulated densities for the three model systems are listed in Table 2. When the density of model A is plotted against temperature as shown in Figure 3, the density of the model polymer increases with decreasing the temperature. The PE with 200 carbons in the chain backbone, which behaves like a dense PE, is not amorphous liquid at below room temperature.[20] Therefore, the experimental densities of amorphous PE at 50−300 K are not readily available. The densities at those temperatures can be only estimated from the melt densities at high temperatures. The simulated densities

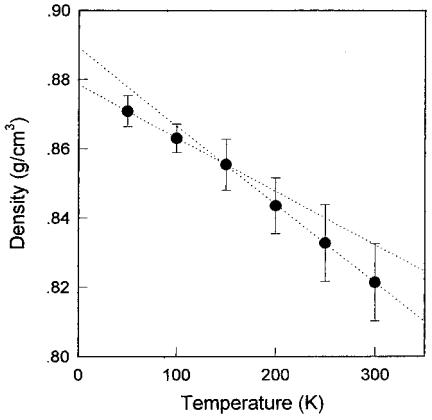

Figure 3. Temperature dependence of the density for model A. A discontinuity of the slope is observed at 150 K.

at 300 K are lower than the experimentally estimated ones, whereas the linear thermal expansion coefficient above 150 K agree well with experimental values, as seen in Table 2. Such lower values of densities from simulation have been reported for several other polymers.[23] There is a discontinuity in the thermal expansion coefficient at 150 K as can be seen in Figure 3. The temperature corresponds to the experimental γ-transition temperature of PE. It may be immature to assign the break point as the real glass transition because of the unrealistic high cooling rate adopted here (−1 K/ps). Nevertheless, the simulation results by other workers also report the same observation for the break point.[19]

Table 3 and Figure 4 show the total energies as functions of temperature. The kinetic energy extrapolated to 0 K is about 0, which is reasonable because the energy is defined by the velocities of atoms in a system. The thermal motion ceases at 0 K. Therefore, the total energy at 0 K becomes equal to the potential energy at 0 K. The charges distributed in this polymer, which has only carbons and hydrogens, do not have the attractive attribute, and thus the electrostatic energy is positive at all temperatures. The model C polymer has a nonzero positive value of electrostatic energy, although the value is small compared to the van der Waals energy in magnitude. Consequently, the total energy becomes lower than that of model A and model B in its magnitude, which may result in lower cohesive energy density if there is no corresponding volume contraction. The solubility parameters are calculated at 300 K from the cohesive energy density and listed in Table 4. The cohesive energy density is calculated by subtracting the total energy at bulk state from the total energy of a single chain in vacuum and dividing the difference by the volume,[24] since the cohesive energy density is defined as the energy difference when a material of unit volume is vaporized. The simulated solubility param-

Table 2. Densities Obtained by MD

	density (g/cm^3)			
T (K)	model A	model B	model C	exptl
50	0.870 ± 0.004	0.872 ± 0.004	0.874 ± 0.003	
100	0.863 ± 0.004	0.865 ± 0.004	0.866 ± 0.004	
150	0.855 ± 0.007	0.856 ± 0.005	0.860 ± 0.007	
200	0.843 ± 0.008	0.845 ± 0.009	0.848 ± 0.006	
250	0.832 ± 0.011	0.832 ± 0.006	0.833 ± 0.006	
300	0.821 ± 0.011	0.823 ± 0.010	0.828 ± 0.008	0.857,[a] 0.855,[b] 0.847[c]
linear thermal expansivity (10^{-4} K^{-1})	0.92[d]	0.90[d]	0.89[d]	1.0[b]

[a] Extrapolated from the experimental densities of C_{142}[20] above melting temperature to obtain the densities in amorphous state. [b] From ref 21. [c] From ref 22. [d] From data above 150 K.

Table 3. Energies Obtained by MD

	T (K)	total E	potential E	kinetic E	nonbonded E	valence E	bond E	angle E	torsion E	vdW E	Coulomb E
model A	50	65.3 ± 14.1	−27.2 ± 14.1	92.5 ± 2.1	−260.5 ± 6.6	233.4 ± 7.9	67.1 ± 2.1	125.0 ± 6.3	41.3 ± 0.5	−260.5 ± 6.6	0.0 ± 0.0
	100	241.4 ± 11.7	63.3 ± 13.0	178.1 ± 1.8	−247.7 ± 3.9	311.0 ± 9.5	97.2 ± 1.8	169.3 ± 7.3	44.5 ± 1.1	−247.7 ± 3.9	0.0 ± 0.0
	150	414.8 ± 17.9	150.5 ± 15.5	264.3 ± 4.3	−233.2 ± 5.3	383.7 ± 11.1	127.9 ± 4.1	210.2 ± 8.1	45.7 ± 0.7	−233.2 ± 5.3	0.0 ± 0.0
	200	598.8 ± 14.2	246.5 ± 16.7	352.4 ± 2.9	−219.9 ± 10.2	466.3 ± 6.7	161.2 ± 2.1	257.0 ± 7.6	48.2 ± 0.8	−219.9 ± 10.2	0.0 ± 0.0
	250	783.6 ± 13.9	342.5 ± 16.8	441.1 ± 4.2	−201.5 ± 8.7	544.1 ± 11.6	192.1 ± 6.6	297.3 ± 6.8	54.6 ± 1.9	−201.5 ± 8.7	0.0 ± 0.0
	300	969.6 ± 11.8	441.7 ± 10.7	527.9 ± 4.2	−181.4 ± 6.4	623.1 ± 5.1	225.7 ± 5.7	339.6 ± 11.5	57.9 ± 4.2	−181.4 ± 6.4	0.0 ± 0.0
model B	50	49.8 ± 12.3	−41.8 ± 13.1	91.6 ± 1.3	−273.7 ± 5.5	231.9 ± 7.6	65.8 ± 1.1	124.7 ± 6.2	41.4 ± 0.8	−273.7 ± 5.5	0.0 ± 0.0
	100	224.1 ± 11.1	46.8 ± 12.9	177.3 ± 2.2	−261.3 ± 4.6	308.1 ± 8.6	98.2 ± 2.4	166.8 ± 6.1	43.1 ± 0.8	−261.3 ± 4.6	0.0 ± 0.0
	150	402.1 ± 10.4	139.2 ± 14.1	262.9 ± 4.5	−247.2 ± 5.6	386.5 ± 9.2	127.7 ± 2.4	212.1 ± 6.8	46.7 ± 0.7	−247.2 ± 5.6	0.0 ± 0.0
	200	594.2 ± 23.0	237.8 ± 18.1	356.4 ± 5.1	−232.4 ± 9.6	470.2 ± 8.8	161.6 ± 2.2	258.4 ± 8.1	50.2 ± 0.8	−232.4 ± 9.6	0.0 ± 0.0
	250	777.1 ± 27.0	330.0 ± 19.7	447.1 ± 8.0	−210.1 ± 2.7	540.1 ± 20.7	190.6 ± 4.7	296.5 ± 16.4	53.0 ± 1.3	−210.1 ± 2.7	0.0 ± 0.0
	300	971.5 ± 32.8	433.6 ± 25.0	538.0 ± 8.0	−191.9 ± 9.5	625.4 ± 15.8	222.3 ± 4.3	345.8 ± 8.3	56.9 ± 4.3	−191.8 ± 9.5	0.0 ± 0.0
model C	50	76.0 ± 24.0	−14.1 ± 23.0	90.2 ± 1.1	−233.6 ± 13.1	219.4 ± 9.9	63.8 ± 1.8	109.7 ± 7.4	45.9 ± 0.8	−253.9 ± 4.5	20.3 ± 8.6
	100	256.7 ± 30.5	77.5 ± 26.2	179.2 ± 4.4	−218.0 ± 13.3	295.6 ± 13.0	94.7 ± 4.0	152.7 ± 8.9	48.1 ± 0.2	−239.6 ± 4.2	21.5 ± 9.2
	150	427.3 ± 24.2	167.1 ± 23.7	260.1 ± 2.4	−205.3 ± 17.0	372.5 ± 7.0	127.2 ± 1.5	194.9 ± 6.3	50.3 ± 0.8	−228.6 ± 7.7	23.2 ± 9.4
	200	618.3 ± 36.8	267.3 ± 35.2	351.1 ± 2.2	−176.9 ± 28.0	444.3 ± 7.7	155.5 ± 2.3	234.1 ± 8.1	54.6 ± 0.6	−211.0 ± 4.9	34.0 ± 23.2
	250	804.8 ± 44.4	364.9 ± 44.1	439.2 ± 1.5	−159.7 ± 32.9	524.7 ± 11.5	184.4 ± 2.0	283.5 ± 10.7	56.8 ± 1.7	−193.2 ± 10.0	33.3 ± 22.9
	300	982.4 ± 36.1	457.3 ± 41.7	525.0 ± 6.3	−146.9 ± 27.2	604.3 ± 14.8	217.9 ± 2.9	323.8 ± 14.0	62.5 ± 1.7	−180.0 ± 4.8	33.0 ± 23.3

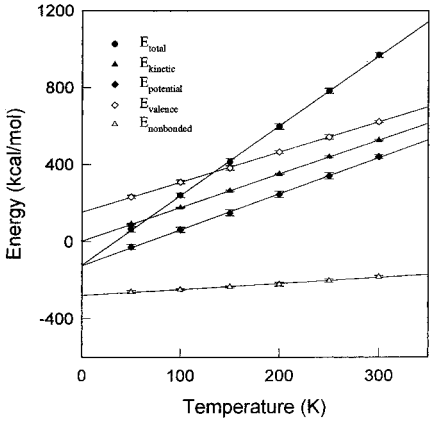

Figure 4. Temperature dependence of the total energies for model A where $E_{total} = E_{potential} + E_{kinetic}$ and $E_{potential} = E_{nonbonded} + E_{valence}$.

Table 4. Solubility Parameters (cal/cm^3)$^{1/2}$ Obtained by MD

model A	model B	model C	exptl[a]
7.78 ± 0.18	7.94 ± 0.42	7.48 ± 0.75	7.91

[a] From ref 21.

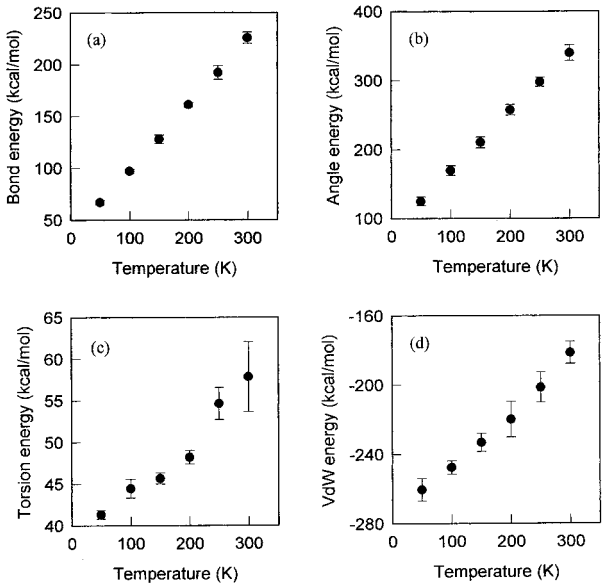

Figure 5. Temperature dependence of the energy components for model A: (a) bond energy; (b) angle energy; (c) torsional energy; (d) van der Waals energy. A nonlinear behavior is observed in the plot of torsion energy *vs* temperature, which seems to be related to the γ-transition of PE.

eters are in good agreement with the experimental value.

A discernible evidence of a transition can not be found easily in Figure 4. A discontinuity, however, is observed when the torsional energy is plotted against temperature as shown in Figure 5, while the other energy components show the linearity over all temperature ranges. Rigby and Roe[25] reported that torsional energy is closely related to a glass transition. Thus the discontinuity of torsional energy at 150 K in our simulation may provide additional evidence for the glass transition.

As a method to analyze the free volumes, the Voronoi tessellation[26] is adopted. Voronoi polyhedra are defined as the minimum polyhedra with the faces which perpendicularly bisect the lines connecting all pairs of atoms. Every point within the polyhedron is therefore

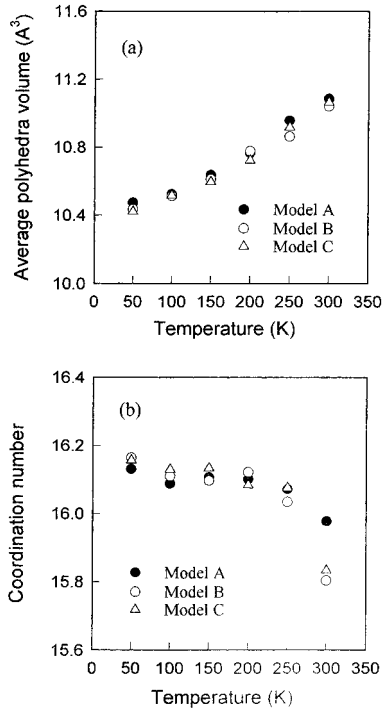

Figure 6. Temperature dependence of (a) the average polyhedra volume and (b) the coordination number calculated from Voronoi tessellation. The volume contains the core volume of an atom and free volume around it.

Table 5. List of Calculated EOS Parameters

		p^* (MPa)	v_{sp}^* (cm^3/g)	T^* (K)
MD	model A	341.3[a]	1.138[a]	614.6
	model B	371.1	1.135	613.9
	model C	326.6	1.136	638.5
MM	model A	318.2 ± 4.6	1.131 ± 0.008	595.2
	model B	335.4 ± 4.8	1.130 ± 0.008	599.8
	model C	306.1 ± 1.9	1.129 ± 0.009	616.8
	exptl range[b]	300−495	1.08−1.14	535−725

[a] Extrapolated from the MD data at 50−150 K. [b] From ref 21.

closer to the chosen atom than to any other atom in the system. The polyhedron will contain both the atom and surrounding free volumes. A coordination number is defined as the number of faces of the polyhedra. In Figure 6, a transition near 150 K may be observed for both the polyhedra volume and the coordination number. These results also support that the transition at 150 K is closely related to the glass transition temperature. The increase of the polyhedra volume and the decrease of the coordination number with the temperature can be easily understood. As the temperature is lowered, the volume contracts, and thereby the number of neighbors around atoms increases.

The data of the close-packed state can be either collected from the MD results, or obtained directly by MM. The cohesive energy density at 0 K corresponds to p^*, and the specific volume at 0 K to v_{sp}^*. The characteristic temperature T^* is obtained by inserting p^*, v_{sp}^*, and simulated (T, v) data into the LF EOS theory. The characteristic parameters are listed in Table 5, which are comparable to the experimentally determined values. The segmental core volume $v^* = kT^*/p^*$ is equal to 22.8 Å^3 and the degree of polymerization, 100, corresponds to the molecular size parameter (r) of 231.7 for the MD results of model B. Thus, the fourth term in the rhs of eq 1 vanishes for this C_{200}

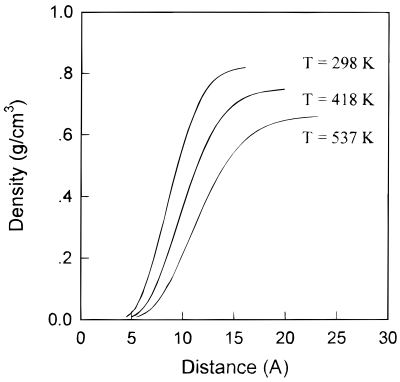

Figure 7. Density profiles at the surface, which are calculated numerically based on eq 4 at several temperatures with the simulated equation-of-state parameters obtained from MD for model B.

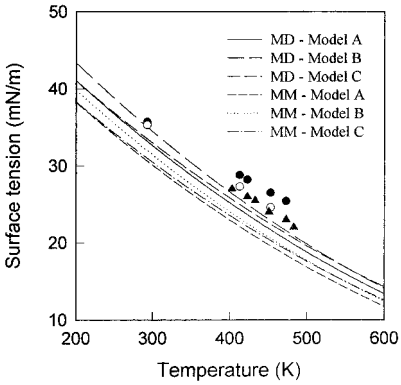

Figure 8. Temperature dependence of surface tensions (lines), which is calculated numerically based on eq 5, using the simulated equation-of-state parameters listed in Table 4. The symbols represent the experimental data: (●) linear PE, mw = 67000;[27] (○) branched PE, mw = 7000;[27] (▲) C_{150}, mw = 2100.[28]

system. Substituting the simulated characteristic parameters into eqs 4 and 5 leads to the density profiles at surface and the surface tensions as functions of temperature, respectively. Figure 7 and Figure 8 show the density profiles at the surface and the temperature dependence of the surface tensions, respectively. The best prediction of surface tension is obtained when the parameters from the MD simulation for model B are used. The exact calculation method of the long-range interaction is important, and the positive Coulomb energy of model C may reduce the cohesive energy density and the surface tension. The MD results show better efficiency in building relaxed structures, although much longer simulation time is consumed. The calculated surface tensions without adjustable parameters are slightly underestimated as compared to the experimental measurements, as shown in Figure 8. This underestimation may come from two sources. One is lower values of simulated densities due to the loose packing of the model structure. The absence of crystallization in our simulations may yield lower density at the close-packed structure, resulting in lower cohesive energy density, and thereby lower surface tension. Another is the ambiguity of EOS parameters. According to the concept of the original theory, the EOS characteristic parameters must be determined only as material properties, but the values become dependent upon temperature when the theory is fitted to experimental data to obtain the EOS parameters. In our simulations, the EOS characteristic parameters determined from the data below 300 K have been used for calculating the

surface tension, although the parameters are, in reality, functions of temperature. The use of such data may cause the discrepancy between simulation and experiment.

The surface of polypropylene was studied by Mansfield and Theodorou.[29−31] They built the surface structures by adopting the united atom model and performing the MC, MM, and MD. They calculated the internal energy contribution to the surface tension by subjecting the model system to a small deformation dilating the surface area, relaxing anew, and monitoring the change in potential energy at the minimum. Cifra and Nies[32,33] have also calculated the surface tension and surface density profile of several polymers as functions of temperature by means of the lattice MC simulation. However, they did not attempt to determine the EOS parameters from their simulations. They used the experimentally determined EOS parameters to calculate the surface tension from the EOS theory and then compared the simulation results with the EOS prediction.

The principal merit of our method lies in that the application can be simply extended to other research areas such as the phase behavior of multiphase polymer systems[34] and the interfacial tensions between immiscible polymer blends, as long as such behaviors can be properly described by the EOS theory, because our method provides a way to determine the EOS parameters without any experimental effort.

Conclusions

The equation-of-state parameters p^*, v_{sp}^*, and T^* of polyethylene have been calculated by molecular simulations, without any experimental effort. The values were in the range of the experimentally determined ones. With the calculated parameters, the surface tensions and surface density profiles were obtained by numerically integrating the Poser and Sanchez equation. The calculated values of surface tension without adjustable parameters are slightly underestimated compared with the experimental ones, which may arise from two sources: One is lower values of simulated densities as compared to the experimental ones and another is inaccuracy of the EOS theory itself. The simulations have been performed in an amorphous state and show a transition phenomenon corresponding to the γ-transition of polyethylene from the change in the volume and the torsional energy. Combining the EOS theory and molecular simulations may provide a new way to predict and to analyze the surface properties of polymers.

Acknowledgment. The authors thank Cheil Industries, Inc. for their financial support.

References and Notes

(1) Allen, M. P.; Tildesley, D. J. *Computer Simulation of Liquids*; Clarendon Press: Oxford, England, 1987.
(2) Monnerie, L., Suter, U. W., Eds. *Advances in Polymer Science 116*; Springer-Verlag: Berlin, 1994.
(3) Burtkert, U.; Allinger, N. L. *Molecular Mechanics*; American Chemical Society: Washington, DC, 1982.
(4) Roe, R. J., Ed. *Computer Simulation of Polymers*; Prentice-Hall: Englewood Cliffs, NJ, 1991.
(5) Binder, K.; Heermann, D. W. *Monte Carlo Simulation in Statistical Physics*; Springer-Verlag: Berlin, 1988.
(6) Baschnagel, J.; Binder, K.; Paul, W.; Laso, M.; Suter, U. W.; Batoulis, I.; Jilge, W.; Bürger, T. *J. Chem. Phys.* **1991**, *95*, 6014.
(7) Kim, Y.-H.; Nelson, J. T.; Glynn, A. B. *Cereal Foods World* **1994**, 39, 8.
(8) Honeycutt, J. D. *Macromolecules* **1994**, *27*, 5377.
(9) Fan, C. F.; Olafson, B. D.; Blanco, M.; Hsu, S. L. *Macromolecules* **1992**, *25*, 3667.
(10) Tao, H.-J.; Fan, C. F.; MacKnight, W. J.; Hsu, S. L. *Macromolecules* **1994**, *27*, 1720.
(11) Sanchez, I. C. In *Polymer Blends*; Paul, D. R., Ed.; Academic Press: New York, 1978.
(12) Poser, C. I.; Sanchez, I. C. *J. Colloid Interface Sci.* **1979**, *69*, 539.
(13) Sanchez, I. C. In *Physics of Polymer Surfaces and Interfaces*; Sanchez, I. C., Ed.; Butterworth-Heinemann, 1992.
(14) Sanchez, I. C.; Lacombe, R. H. *J. Phys. Chem.* **1976**, *80*, 2352.
(15) Rappé, A. K.; Casewit, C. J.; Colwell, K. S.; Goddard, W. A., III; Skiff, W. M. *J. Am. Chem. Soc.* **1992**, *114*, 10024.
(16) Rappé, A. K.; Goddard, W. A., III. *J. Phys. Chem.* **1991**, *95*, 3358.
(17) Berendsen, H. J. C.; Postma, J. P. M.; van Gunsteren, W. F.; DiNola, A.; Haak, J. R. *J. Chem. Phys.* **1984**, *81*, 3684.
(18) Boyd, R. H.; Pant, P. V. K. *Macromolecules* **1991**, *24*, 4073.
(19) Boyd, R. H.; Pant, P. V. K. *Macromolecules* **1991**, *24*, 4078.
(20) Dee, G. T.; Ougizawa, T.; Walsh D. J. *Polymer* **1992**, *33*, 3462.
(21) Brandrup, J., Immergut, E. H., Eds. *Polymer Handbook*, 3rd ed.; John Wiley & Sons: New York, 1989.
(22) Maloney, D. P.; Prausnitz, J. M. *J. Appl. Polym. Sci.* **1974**, *18*, 2703. Calculated from eq 1 of this paper.
(23) Vasudevan, V. J.; McGrath, J. E. *Macromolecules* **1996**, *29*, 637 and references therein.
(24) Theodorou, D. N.; Suter, U. W. *Macromolecules* **1985**, *18*, 1467.
(25) Rigby, D.; Roe, R. J. *J. Chem. Phys.* **1987**, *87*, 7285.
(26) Rigby, D.; Roe, R. J. *Macromolecules* **1990**, *23*, 5312.
(27) Wu, S. *Polymer Interface and Adhesion*; Marcel Dekker, Inc.: New York, Basel, 1982.
(28) Dee, G. T.; Sauer, B. B. *J. Colloid Interface Sci.* **1992**, *152*, 85.
(29) Mansfields, K. F.; Theodorou, D. N. *Macromolecules* **1989**, *22*, 3143.
(30) Mansfields, K. F.; Theodorou, D. N. *Macromolecules* **1991**, *24*, 6283.
(31) Mansfields, K. F.; Theodorou, D. N. In *Computer Simulation of Polymers*; Roe, R. J., Ed.; Prentice-Hall: Englewood Cliffs, NJ, 1991.
(32) Cifra, P.; Nies, E.; Karasz, F. E. *Macromolecules* **1994**, *27*, 1166.
(33) Nies, E.; Cifra, P. *Macromolecules* **1994**, *27*, 6033.
(34) Choi, K.; Jo, W. H.; Hsu, S. L. Manuscript in preparation.

MA9600419